JTTEE5 18:58–64
DOI: 10.1007/s11666-008-9247-4
1059-9630/$19.00 © ASM International

Indentation of Metallic and Cermet Thermal Spray Coatings

W.B. Choi, L. Prchlik, S. Sampath, and A. Gouldstone

(Submitted August 29, 2007; in revised form August 5, 2008)

Indentation methods are presented by which the elastic and inelastic stress-strain characteristics of metallic thermal spray (TS) coatings on substrates may be extracted. The methods are based on existing techniques for brittle solids, and adapted for the finite geometry associated with coatings. Basic assumptions and derivations are given, along with guidelines for experimental measurement. Using these, indentation inelastic stress-strain curves are generated for NiCrAlY and Ni-Al bondcoats, as well as WC-Co cermet coatings. Elastic moduli are extracted for CoNiCrAlY coatings. Results are briefly discussed in the context of the effect of feedstock material, process and post-process heat treatment on the intrinsic properties of splats as well as their in-coating cohesion. The methods presented are attractive, particularly for the TS industry, due to the minimal specimen preparation and lack of intricate equipment required for measurement.

Keywords bondcoat, cohesion, indentation testing, inelastic, modulus

1. Introduction

Structure and properties of thermal spray (TS) coatings are very sensitive to spray method, input parameters, powder morphology, and environment. For a long time, this complex relationship limited expansion of TS into prime-reliant applications, that is to say, in which coating failure leads to component failure. Progress in process control in the past decade has increased the potential for coating design, and insertion of TS into non-traditional applications. Along with such improvements, the TS community has begun using next-generation characterization techniques. For example, 3D imaging using tomography and scattering techniques provides microstructural information beyond that obtained with conventional cross-sectional image analysis (Ref 1-5). In situ substrate curvature experiments and diffraction techniques have illustrated the development of coating stresses during deposition and post-process annealing (Ref 6).

Significant progress has been made in indentation testing as well; such measurements have evolved beyond conventional hardness testing, for example to extract coating elastic modulus. In the literature, three primary methods for modulus measurement have been reported. Instrumented indentation is being adopted rapidly, using the Oliver-Pharr method (Ref 7). Knoop indentation allows modulus extraction via measurement of elastic recovery of the imprint minor diagonal (Ref 8). Scratch tests under spherical contact on a gold-coated surface reveal a contact surface that increases with increasing load, and modulus can be fit via Hertzian relations (Ref 9). The first two methods require unloading of the indenter, following inelastic deformation of the probed material; such inelasticity, if non-conservative, could affect modulus. (For example, micro cracking would lower modulus and pore compaction would increase it.) In addition, a single data point arises from each test, and a linear elastic behavior is assumed. As coatings have shown non-linear elastic behavior in a number of studies (e.g., Ref 10) this assumption can lead to errors. Finally, instrumented indenters may be too costly for a typical metallographic laboratory. The third method allows the 'undamaged' modulus to be measured, but requires tangential motion of the tip, and the contact area is difficult to measure at low loads (Ref 9). Accordingly, here we describe an adapted method to extract elastic modulus of coatings, using a hardness tester under normal loading, addressing the above concerns. In addition, we show a similar method to measure high-strain inelastic properties.

Contact methods, namely indentation, are ideally suited for the mechanical probing of TS coatings due to the minimal specimen preparation involved and ability to conduct multiple tests on a single sample. Instrumented indentation has received major attention in the mechanics literature, with a number of papers on the analysis of load-depth (P-h) curves for the extraction of yield point and hardening behavior of materials (Ref 11-16). Application of such analyses and models to TS coatings is limited, however, as for the most part they assume von Mises behavior, and in some cases property extraction can be laborious. In addition, industrial usage, particularly for small 'job shops' is hindered by the cost of instrumented indenters. Another method, adapted from Brinell hardness measurements, has been used to extract inelastic

W.B. Choi, L. Prchlik and **S. Sampath**, Center for Thermal Spray Research, State University of New York, Stony Brook, NY; and **A. Gouldstone**, Department of Mechanical and Industrial Engineering, Northeastern University, Boston, MA. Contact e-mail: bubbleraft@gmail.com.

(and to a lesser extent, elastic) properties of ceramic materials, and brittle matrix composites (e.g., Ref 17). However, these tests have not been used to look at the intrinsic properties of TS coatings (neglecting the substrate). Here, we follow the necessary adaptations, and show some experiments and results for four illustrative materials, namely Ni-Al, NiCrAlY, and CoNiCrAlY bondcoats (Ref 18), and WC-Co cerrmet coatings. Inelastic behavior for the first two of these is critical for the operation of thermal barrier coatings (TBCs); yielding of bondcoats is directly related to propensity for rumpling and thus TBC spallation (Ref 19). For the latter, high-strain inelastic properties provide insight into the important problems of wear, erosion, and foreign object damage (Ref 20-24).

2. Background of Methods

2.1 Inelastic Properties

We discuss inelastic properties first because they are more easily obtained, and the method is used more here. The goal of such tests is to extract an equivalent 'stress-strain' curve akin to a uniaxial compression test (Ref 25). Under indentation loading, deformation is non-uniform and analysis thus becomes more complex relative to uniaxial testing. Analytical solutions (for displacements, strains, stresses) for a homogeneous material within its elastic limit are available in the literature, but under elastic-inelastic straining such closed-form descriptions do not exist. To address this, Tabor showed that underneath a spherical indenter of radius R the contact pressure is influenced by the degree of imposed strain, and this has been followed by others (Ref 16, 25). He also introduced the concept of so-called representative strain, ε_R that is related to the average strain around the indenter. As shown in Fig. 1, this is given by the relation

$$\varepsilon_R = 0.2\frac{a}{R} \qquad \text{(Eq 1)}$$

where a and R are contact and indenter radii, respectively. Similarly, contact flow stress σ_{flow} was determined empirically to be

$$\sigma_{flow} = \frac{pm}{2.8} \qquad \text{(Eq 2)}$$

where the mean pressure $pm = P/\pi a^2$, P being indentation load.

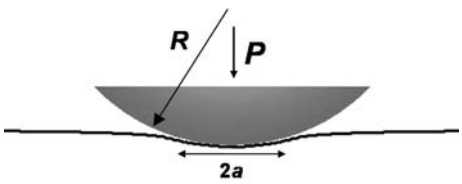

Fig. 1 Schematic of spherical (Hertzian) indentation with a tip of radius R, showing contact dimensions

It is apparent from the above two relations that spherical indentation with successively larger load P, combined with observation of resulting contact radii, can be employed to construct an illustrative 'stress-strain' curve for the indented material. Such data could be extracted using three primary methods:

(1) analysis of continuous P-h curves provided by commerically available instrumented indenters,
(2) analysis of continuous P-h curves provided by custom-built instrumented indenters (i.e., fixtures on a mechanical testing frame),
(3) analysis of an array of surface imprints created by a hardness tester, whereby contact diameter $2a$ is measured optically.

Method 1 is used for bulk materials and thin films (Ref 14). Method 2 has been used previously to extract composite properties of coatings on substrates, for the assessment of behavior under high-load contact (Ref 26, 27). Here we use Method 3—Metallographic hardness testers often have a wide load range (10-500 N), allowing high inelastic strains to be achieved in large sample volumes. In addition, they are relatively inexpensive to obtain (if not pre-existing in most metallographic laboratories), easily adaptable, and simple to operate and maintain. A lower number of data points is generated than in the case of continuous indentation. In addition, the resulting impression represents residual deformation, as opposed to deformation at maximum load. However, this latter concern can be overcome by the application of a thin gold coating sputtered on the surface of the specimen (e.g., Ref 17), which reveals impression at maximum load.

2.2 Elastic Properties

Elastic properties (e.g., elastic modulus) of TS coatings are usually probed via the instrumented indentation technique that continuously presses a rigid tip into the specimen, and measures P versus h. The elastic modulus is extracted from unloading portion of the P-h curve via the well-known Oliver-Pharr method (Ref 7). Dead-weight indentation methods may be used to extract elastic properties of materials; the crucial step is to capture the contact dimensions at maximum load by depositing a thin gold film on the surface of the specimen. The specimen is then pressed with a sphere, and though the deformation is nominally elastic, the film deforms or rubs off. If one considers the indentation by an elastic sphere of radius R, the defining equations are:

$$p_m = \frac{2}{3}\left(\frac{6PE^{*2}}{\pi^3 R^2}\right)^{\frac{1}{3}} = \frac{P}{\pi a^2} = \frac{2}{3}p_o \qquad \text{(Eq 3)}$$

$$\frac{1}{E^*} = \frac{1-\upsilon_S^2}{E_S} + \frac{1-\upsilon_i^2}{E_i} \qquad \text{(Eq 4)}$$

Where E_S, E_i, υ_S, and υ_i are elastic modulus and Poisson's ratio of sample and indenter, respectively. The term p_o is

the maximum Hertzian pressure, and is given as a Ref 28.

From Eq 3, it is apparent that a plot of contact pressure p_m versus maximum load P, within the elastic limit, can be fit to provide E^*. Contact pressure may be calculated by recording the contact diameter $2a$, left in the deformed gold film, and performing the necessary arithmetic. Upon yielding, the material becomes more compliant, and pressure versus load deviates from the theoretical elastic curve in Eq 3. However, examination of literature measurements show that this measurement works much better under rubbing or scratching (e.g., Ref 9), as a tangential load is applied to the gold film; normal load indentation has *previously* been less successful, as clear images of the deformed region are difficult to achieve. In addition, no success has *previously* been shown in using this for porous materials like TS coatings. Here we will show a simple adaptation that allows normal loading to be used.

3. Experimental

3.1 Coating Production and Microstructure

Four sets of coating materials were selected for this study (Ref 29). The first set were CoNiCrAlY bondcoats deposited by atmospheric plasma spray and high velocity oxygen fuel (HVOF). The second set of specimens included NiCrAlY bondcoats deposited by atmospheric plasma spray. A sampling of these coatings was also annealed at 850 °C for 1.5 h in air. The two sets of MCrAlY bondcoats were samples obtained from the SUNY-based *Consortium on Thermal Spray Technology*. For the third set of specimens, Ni-5% Al coatings were deposited on steel substrates with four different TS techniques: HVOF, Cold Spray, APS, and Wire Arc. Cross-sectional SEM micrographs of the Ni-5% Al and NiCrAlY coatings are shown in Fig. 2 and 3. For the Ni-5% Al coatings, porosity was measured with mercury intrusion porosimetry (MIP) of all to be less than 6% (Ref 29). A third sample of a HVOF WC-Co cermet coating was also evaluated. Coatings were polished to 1-μm diamond suspension in preparation for indentation. All the coatings tested in this study were close to 400 μm thick, except the Ni-5% Al coatings which were 1 mm thick. In our experiments, polishing within machine parameters had negligible effect on mechanical behavior. Data shown here was limited by availablity of coating specimens.

3.2 Gold Film Deposition

Before indentation a thin (10-20 nm) gold film was sputter deposited on the surface of specimens using a BOC Edwards SEM sputter system to improve visibility of resulting imprints. The distance between sample and the incoming flux was less than 100 mm. Typically, this is done by placing the specimen flat in the chamber. However, our experiments showed that a film deposited in this way showed very poor contrast when pressed. It has been shown that during such physical vapor deposition (PVD) processes, tilting of the specimen results in a shadowing effect, that is to say, the resulting film is porous as film island buildup blocks adjacent deposition (e.g., Ref 30).

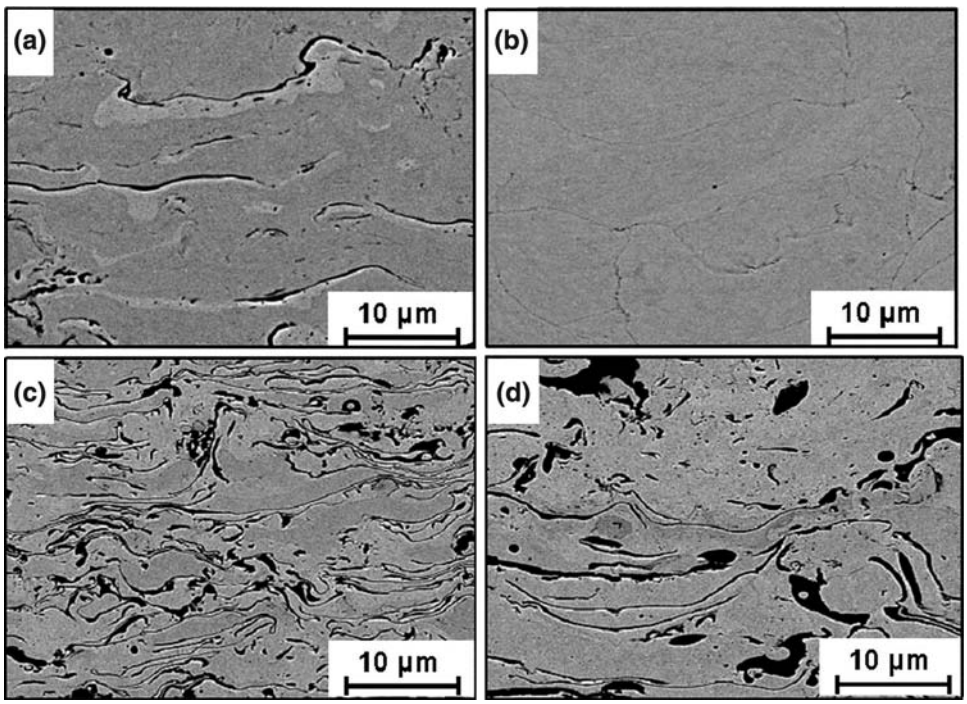

Fig. 2 Cross-sectional SEM micrographs of Ni-5% Al coatings used in the experiments: (a) HVOF; (b) Cold Spray; (c) APS; and (d) Wire Arc

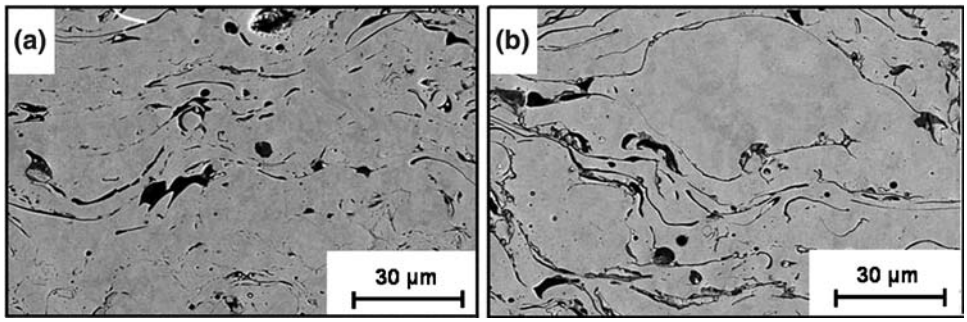

Fig. 3 Cross-sectional SEM micrographs of NiCrAlY (a) as-sprayed and (b) annealed at 850 °C for 1.5 h

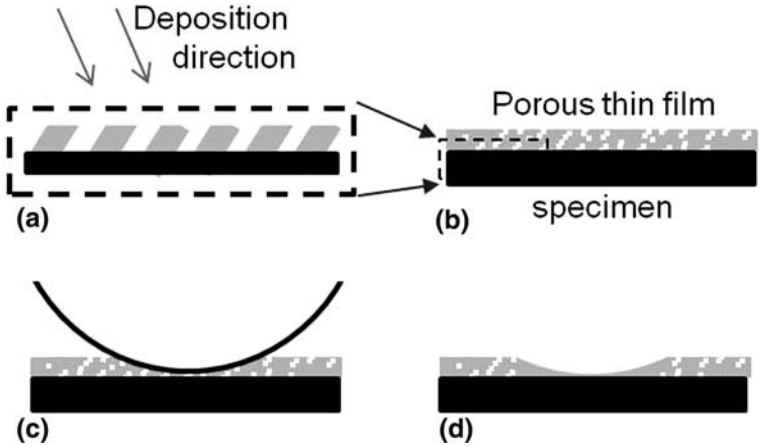

Fig. 4 Schematic of the gold-coating process allowing better visualization of indents. (a) Deposition at an angle leads to 'shadowing' between deposited features; this leads to (b) a porous thin film. (c) Indentation of this film readily crushes the pores and (d) leaves an imprint that is visible under optical microscopy

We found that tilting the specimen between 2 and 5 degrees during gold PVD provides remarkably good contrast between 'pressed' and 'unpressed' gold film. Figure 4 shows a schematic of this. This also works quite well for some porous materials like TS coatings. This is an important experimental variation, as without it, indents are not measureable.

3.3 Indentation Tests and Analysis

The gold-coated sample was indented using a Buehler Micromet II microhardness tester with a range of eight different loads from 10 mN to 10 N. The samples were then pressed for 20 s with spherical indenters, made with WC-Co spheres of 5/32″ (4 mm) and 3/8″ (9.5 mm) in diameter (McMaster-Carr Grade C-1/C-2). Each indent was analyzed with a Nikon Epiphot 200 metallurgical microscope with Nomarski Diffraction Interference Contrast (DIC) illumination, enhancing the depth contrast. The diameter of imprints was measured with University of Texas Health Science Center at San Antonio (UTHSCSA) Image Tool 3.0 imaging software. When using Eq 4 to extract specimen modulus E_s, the following values were used: $E_i = 714$ GPa, $\nu_i = 0.19$, $\nu_s = 0.3$. For method verification, several bulk (Stainless Steel 304) and

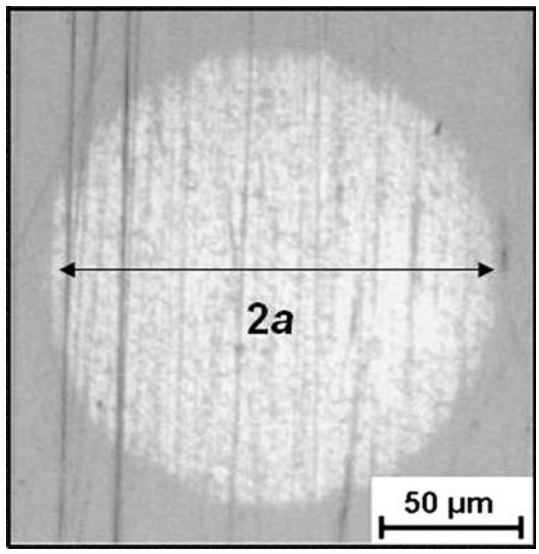

Fig. 5 Optical image of stainless steel 304 imprint left in gold coating after 1N load indentation

TS metallic (HVOF, APS CoNiCrAlY) samples were tested, and moduli compared with known and literature values, or process trends.

All high-strain (inelastic) indentation experiments were performed on a Mitutoyo AVK-2C hardness tester, with a load range of $P = 10$-500 N. Customized spherical tips were assembled by pressing 1/16″ diameter WC-Co spheres (McMaster-Carr) into dimpled brass rods, machined to fit in the tester tip chuck. Specimens were indented five times at each load, and resulting contact diameter $2a$ was measured under optical microscopy for each. Figure 5 shows a representative imprint, under 200× magnification. A typical set of experiments on a specimen lasted approximately 15 min. The effect of indentation hold time (5-30 s) was explored and found to be negligible for these specimens. From the resulting P-a correlations, stress-strain curves were constructed using Eq 1 and 2.

4. Results and Discussion

4.1 Extraction of Elastic Modulus

Figures 6 and 7 show pressure p_m versus load P curves for bulk stainless steel 304 and HVOF and APS CoNiCrAlY, respectively. In the case of bulk stainless steel, data are shown for both the small (5/32″) and large (3/8″) indenters. For the coatings, data is only shown for the large indenter. Data were fit to Eq 3 to give elastic modulus. This was not done using automatic fitting, but rather plotting Eq 3 in a spreadsheet along with the data, and manually selecting E^*; priority was placed on fitting points at lower strains. In all cases a constant elastic modulus was assumed. One justification for this is the relatively low strain to which the coatings were subjected under such indentation. Examination of the upper curve (HVOF) and use of Eq 1 shows a maximum strain of approximately 0.2%, which is in the linear elastic range (Ref 10). In the case of APS, the curve deviates from elasticity at a load of approximately 3 N, corresponding to a strain of 0.2%. Note that in both Figures, any deviation between Eq 3 and the data occurred at the higher loads; also, Eq 3 showed a higher pressure than the data for all deviations. This indicates that above a certain load (as stated above), the material began to inelastically deform, and thus had a higher compliance. Inelastic deformation of TS coatings are contributed by mixed effects of splat interfacial sliding, cracking, dislocations within splats. This argument is sensible as it shows that (for bulk SS) for the same load (above 2 N), yielding occurred for the smaller indenter but not the larger indenter. Obviously, a higher strain and stress would be imparted under the smaller indenter, for the same load. In the case of the coatings, reasonable values of E were obtained in both cases, and it can be seen that the APS coating yields at a lower stress (pressure) than the HVOF. This agrees with literature reports of hardness, etc. (Ref 18, 29).

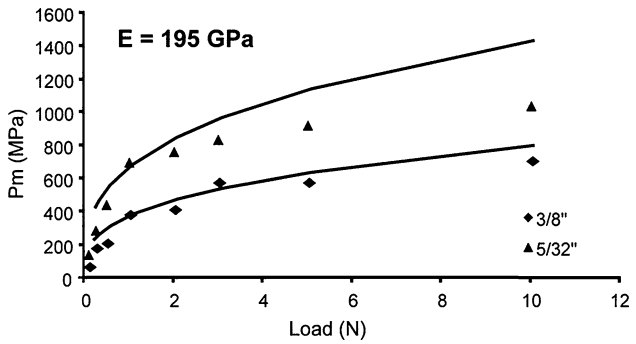

Fig. 6 Elastic modulus of stainless steel 304 as measured via Hertzian indentation and the tilted gold coating technique. Two different size indenters were used for better data fitting

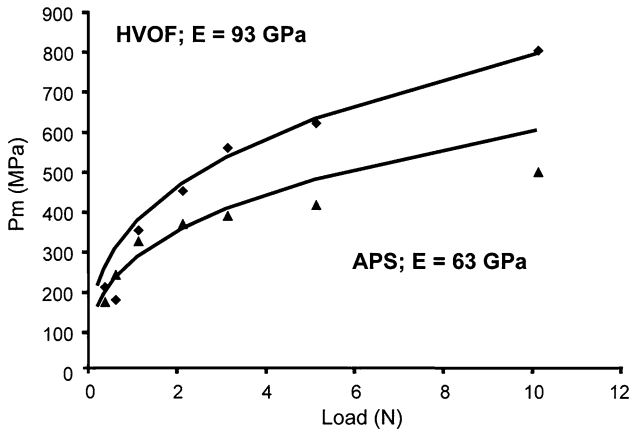

Fig. 7 Elastic moduli of HVOF and APS CoNiCrAlY measured with the tilted gold coating technique. Data only shows indents with 3/8″ indenter in both cases

4.2 NiCrAlY Specimens

Figure 8 shows constructed inelastic stress-strain curves for the NiCrAlY bondcoats in the as-sprayed and annealed condition. The coatings exhibited significant differences in inelastic properties, not only in their absolute values but also in the hardening behavior. Strength increase after heat treatment is at least 300 MPa, and perhaps more significant is the large difference in hardening behavior after heat treatment.

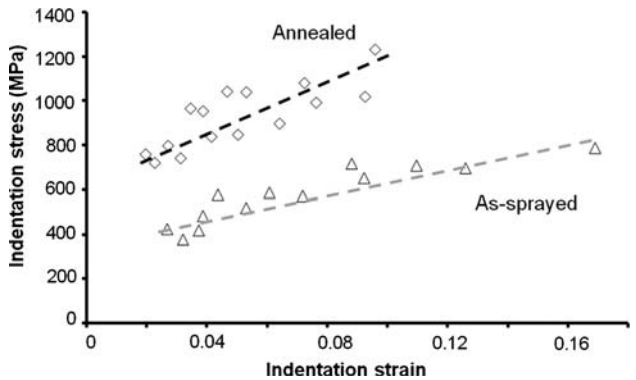

Fig. 8 Indentation stress-strain curves for as-sprayed and annealed NiCrAlY coatings

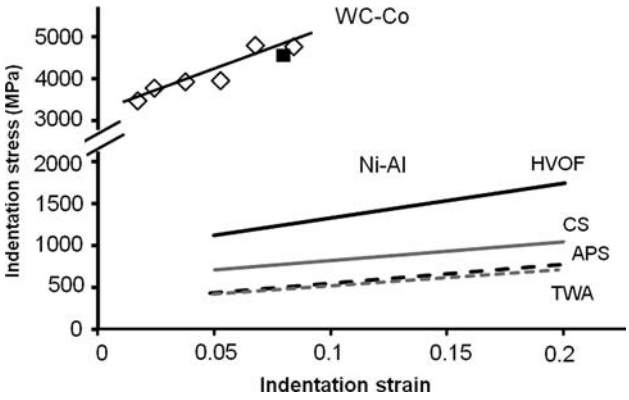

Fig. 9 Indentation stress-strain curves for Ni-5% Al and WC-Co coatings

This result (increase in strength) is not unexpected for TS, as annealing of plasma-sprayed coatings has been shown nearly universally to increase elastic modulus and Vickers microhardness. This is also illustrated in the micrographs of Fig. 3, in which thin interfaces in the as-sprayed specimen (3a) are no longer visible after annealing (3b). However, it is the authors' belief that this is the first time the stress-strain relationship during progression of inelastic deformation has been reported. The higher hardening behavior for the annealed specimens is presumably due to the lowered initial dislocation density after heat treatment, allowing faster multiplication and interaction (Ref 31). In addition, as splat-splat bonding improves due to coalescence of interfaces, intersplat sliding does not contribute as much to inelasticity.

4.3 Ni-Al Specimens

Figure 9 shows constructed inelastic stress-strain curves for the four Ni-Al samples. For the most part, inelastic properties are highly dependent on process (there is fair agreement between the Wire Arc and APS samples). Differences in interfacial characteristics and/or intrinsic splat properties are likely responsible for the variations in stress-strain curves. Differences in hardening slope are not consistent between processes. In other words, as an example the CS curve is offset above the TWA and APS curves, by an approximately constant value. However, the HVOF curve is offset above the CS curve, and hardening slope is increased dramatically. Examining Fig. 2, metallographic examination at this magnification and prediction of properties based on coating 'cleanliness' does not agree with the indentation results.

4.4 WC-Co Specimens

Also plotted in Fig. 9 are the data for the cermet material. Not unexpected, the values are significantly greater than for those of the Ni-Al. For comparison, the single data point corresponding to a Vickers hardness imprint is added, at the characteristic value of 8% strain. The data is presented here to show that meaningful results can be obtained using spherical indentation, even for harder coatings.

5. Conclusions

In this article, we discussed a method, based on Tabor's work, to assess the elastic/inelastic behavior of metallic and cermet TS coatings. This method is simple, allows systematic investigations among different process and post-process parameters, and can be adapted quite easily for, e.g., elevated temperature experiments. In addition, we showed how elastic modulus of coatings might be obtained using a hardness tester. Here it is appropriate to discuss a number of assumptions and guidelines for this method.

(1) In all stress-strain data provided, the measured contact diameter $2a$ was less than one-third of the coating thickness, in order to avoid any substrate effects. This is a suitable rule-of-thumb for such indentation measurements, and is discussed at great length in the open literature. In addition, probe volume was sufficient to measure composite coating properties (Ref 32).

(2) Contact diameter $2a$ was measured via optical microscopy, thus the indentation methods addressed in this study requires good surface optical reflectivity. The gold coating method discussed in this article usually ensures this.

(3) A method was described, based on Hertzian contact theory, to measure the elastic properties of coatings, using a hardness tester. Success of this method hinges upon tilting the sample slightly before application of gold coating for contrast (e.g., Fig. 4) (Ref 30).These methods can readily be employed both for scientific studies as above or in industry as a comparative tool for assessment of coating quality.

Acknowledgments

This work was supported under the National Science Foundation MRSEC Program Award DMR-0080021. A. Gouldstone was supported through NSF CAREER award CMS 0449268.

References

1. A. Kulkarni, Z. Wang, T. Nakamura, S. Sampath, A. Goland, H. Herman, J. Allen, J. Ilavsky, G. Long, J. Frahm, and R.W. Steinbrech, Comprehensive Microstructural Characterization and Predictive Property Modeling of Plasma-Sprayed Zirconia Coatings, *Acta Mater.*, 2003, **51**(9), p 2457-2475
2. J. Ilavsky, G.G. Long, A.J. Allen, and C.C. Berndt, Evolution of the Void Structure in Plasma-Sprayed Ysz Deposits During Heating, *Mater. Sci. Eng., A*, 1999, **272**(1), p 215-221
3. S.H. Leigh and C.C. Berndt, Quantitative Evaluation of Void Distributions Within a Plasma-Sprayed Ceramic, *J. Am. Ceram. Soc.*, 1999, **82**(1), p 17-21

4. T. Keller, W. Wagner, A. Allen, J. Ilavsky, N. Margadant, S. Siegmann, and G. Kostorz, Characterisation of Thermally Sprayed Metallic NiCrAlY Deposits by Multiple Small-Angle Scattering, *Appl. Phys. A: Mater. Sci. Process.*, 2001, **74**, p s975-s977
5. G.G. Long, S. Krueger, and A.J. Allen, Multiple Small-Angle Neutron Scattering, *J. Neutron Res.*, 1999, **7**, p 195-210
6. J. Matejicek and S. Sampath, In Situ Measurement of Residual Stresses and Elastic Moduli in Thermal Sprayed Coatings—Part 1: Apparatus and Analysis, *Acta Mater.*, 2003, **51**(3), p 863-872
7. W.C. Oliver and G.M. Pharr, Measurement of Hardness and Elastic Modulus by Instrumented Indentation: Advances in Understanding and Refinements to Methodology, *J. Mater. Res.*, 2004, **19**(1), p 3-20
8. D. B. Marshall, T. Noma, and A.G. Evans, A Simple Method for Determining Elastic-Modulus-to-Hardness Ratios Using Knoop Indentation Measurements, *J. Am. Ceram. Soc.*, 1982, **65**(10), p C175-C176
9. Y. Xie and H.M. Hawthorne, A Controlled Scratch Test for Measuring the Elastic Property, Yield Stress and Contact Stress-Strain Relationship of a Surface, *Surf. Coat. Technol.*, 2000, **127**(2-3), p 130-137
10. T. Nakamura, G. Qian, and C.C. Berndt, Effects of Pores on Mechanical Properties of Plasma-Sprayed Ceramic Coatings, *J. Am. Ceram. Soc.*, 2000, **83**(3), p 578-584
11. M. Dao, N. Chollacoop, K.J. Van Vliet, T.A. Venkatesh, and S. Suresh, Computational Modeling of the Forward and Reverse Problems in Instrumented Sharp Indentation, *Acta Mater.*, 2001, **49**(19), p 3899-3918
12. T. Nakamura, T. Wang, and S. Sampath, Determination of Properties of Graded Materials by Inverse Analysis and Instrumented Indentation, *Acta Mater.*, 2000, **48**(17), p 4293-4306
13. S.I. Bulychev, V.P. Alekhin, M.K. Shorshorov, A.P. Ternovskii, and G.D. Shnyrev, Determination of Youngs Modulus According to Indentation Diagram, *Zavod. Lab.*, 1975, **41**(9), p 1137-1140
14. Y.T. Cheng and C.M. Cheng, Can Stress-Strain Relationships Be Obtained from Indentation Curves Using Conical and Pyramidal Indenters?, *J. Mater. Res.*, 1999, **14**(9), p 3493-3496
15. M. Beghini, L. Bertini, and V. Fontanari, Evaluation of the Stress-Strain Curve of Metallic Materials by Spherical Indentation, *Int. J. Solids Struct.*, 2006, **43**(7-8), p 2441-2459
16. M.M. Chaudhri, Subsurface Plastic Strain Distribution around Spherical Indentations in Metals, *Philos. Mag. A*, 1996, **74**(5), p 1213-1224
17. B.R. Lawn, Y. Deng, P. Miranda, A. Pajares, H. Chai, and D.K. Kim, Overview: Damage in Brittle Layer Structures from Concentrated Loads, *J. Mater. Res.*, 2002, **17**(12), p 3019-3036
18. V. Higuera, F.J. Belzunce, and J. Riba, Influence of the Thermal-Spray Procedure on the Properties of a Conicraly Coating, *Surf. Coat. Technol.*, 2006, **200**(18-19), p 5550-5556
19. A.G. Evans, D.R. Mumm, J.W. Hutchinson, G.H. Meier, and F.S. Pettit, Mechanisms Controlling the Durability of Thermal Barrier Coatings, *Prog. Mater. Sci.*, 2001, **46**(5), p 505-553
20. L.C. Erickson, H.M. Hawthorne, and T. Troczynski, Correlations Between Microstructural Parameters, Micromechanical Properties and Wear Resistance of Plasma Sprayed Ceramic Coatings, *Wear*, 2001, **250**, p 569-575
21. L.C. Erickson, R. Westergard, U. Wiklund, N. Axen, H.M. Hawthorne, and S. Hogmark, Cohesion in Plasma-Sprayed Coatings—A Comparison Between Evaluation Methods, *Wear*, 1998, **214**(1), p 30-37
22. R.S. Lima, A. Kucuk, and C.C. Berndt, Evaluation of Microhardness and Elastic Modulus of Thermally Sprayed Nanostructured Zirconia Coatings, *Surf. Coat. Technol.*, 2001, **135**(2-3), p 166-172
23. S.W.K. Kweh, K.A. Khor, and P. Cheang, Plasma-Sprayed Hydroxyapatite (Ha) Coatings with Flame-Spheroidized Feedstock: Microstructure and Mechanical Properties, *Biomaterials*, 2000, **21**(12), p 1223-1234
24. Z. Mohammadi, A.A. Ziaei-Moayyed, and A.S.M. Mesgar, Adhesive and Cohesive Properties by Indentation Method of Plasma-Sprayed Hydroxyapatite Coatings, *Appl. Surf. Sci.*, 2007, **253**(11), p 4960-4965
25. D. Tabor, *The Hardness of Metals*, Oxford University Press, Oxford, 1951
26. A. Pajares, L.H. Wei, B.R. Lawn, and C.C. Berndt, Contact Damage in Plasma-Sprayed Alumina-Based Coatings, *J. Am. Ceram. Soc.*, 1996, **79**(7), p 1907-1914
27. A. Pajares, L.H. Wei, B.R. Lawn, N.P. Padture, and C.C. Berndt, Mechanical Characterization of Plasma Sprayed Ceramic Coatings on Metal Substrates by Contact Testing, *Mater. Sci. Eng., A*, 1996, **208**(2), p 158-165
28. K. Johnson, *Contact Mechanics*, Cambridge University Press, Cambridge, UK, 1985
29. S. Sampath, X.Y. Jiang, J. Matejicek, L. Prchlik, A. Kulkarni, and A. Vaidya, Role of Thermal Spray Processing Method on the Microstructure, Residual Stress and Properties of Coatings: An Integrated Study for Ni-5 Wt.%Al Bond Coats, *Mater. Sci. Eng., A*, 2004, **364**(1-2), p 216-231
30. K. Robbie and M.J. Brett, Sculptured Thin Films and Glancing Angle Deposition: Growth Mechanics and Applications, *J. Vac. Sci. Technol. A*, 1997, **15**(3), p 1460-1465
31. R. Abbaschian and R.E. Reed-Hill, *Physical Metallurgy Principles*, Cengage-Engineering, Florence, KY, 1991
32. N. Margadant, J. Neuenschwander, S. Stauss, H. Kaps, A. Kulkarni, J. Matejicek, and G. Rossler, Impact of Probing Volume from Different Mechanical Measurement Methods on Elastic Properties of Thermally Sprayed Ni-Based Coatings on a Mesoscopic Scale, *Surf. Coat. Technol.*, 2006, **200**(8), p 2805-2820